2-1-2001

Tidal Asymmetry in an Estuarine Pycnocline 2. Transport

David A. Jay
Portland State University

Cynthia N. Cudaback

Citation Details

Cudaback, C. N., and D. A. Jay (2001), Tidal asymmetry in an estuarine pycnocline 2. Transport, J. Geophys. Res., 106(C2), 2639â€“2652.

JOURNAL OF GEOPHYSICAL RESEARCH, VOL. 106, NO. C2, PAGES 2639–2652, FEBRUARY 15, 2001

Tidal asymmetry in an estuarine pycnocline 2. Transport

Cynthia N. Cudaback

Marine Science Institute, University of California, Santa Barbara, California

David A. Jay

Environmental Science and Engineering, Oregon Graduate Institute, Beaverton, Oregon

Abstract. Flood currents in shallow estuaries are driven by an along-channel barotropic and baroclinic pressure gradient that increases monotonically toward the bottom, while friction retards near-bottom currents. Therefore, in many estuaries there is a middepth maximum in flood currents. We explore this phenomenon using a simple three-layer model in which each layer has vertically uniform currents and constant density. In this model the middle layer is of intermediate density and grows by shear-induced entrainment from the other two layers. This very simple model produces a middepth maximum in flood currents and simulates observed currents in the Columbia River entrance channel within about 10%. There is good qualitative agreement between model salinity transport and observed transport. The model pycnocline rises and falls tidally, in phase with the observed pycnocline, although pycnocline depth and thickness are better simulated using results from a two-layer model [*Cudaback and Jay*, 2000].

1. Introduction

The transport of water, salt, and nutrients through narrow estuarine channels determines water properties of the estuary and coastal ocean, influences coastal circulation, and impacts the health of many ecosystems. At some stages of the tide this exchange transport is two-layered, seaward at the surface and landward at the bottom. However, on early flood, currents are strongest at middepth. This phenomenon, which is observed in many estuaries [*Geyer*, 1985; *Geyer and Farmer*, 1989; *Cudaback and Jay*, 1996; *Nepf and Geyer*, 1996], reduces along-channel salinity transport relative to the predictions of a two-layer model.

Here we present a new three-layer model of along-channel circulation in an estuarine channel, with the specific goal of studying this middepth velocity maximum on early flood. The along-channel baroclinic pressure gradient drives a current that should increase toward the bottom, while bottom friction retards near-bed currents, so the strongest early flood currents are observed at middepth. In the Fraser River, British Columbia [*Geyer and Farmer*, 1989], as in the Columbia River, this middepth maximum is usually in the pycnocline, although it is seen below the pycnocline in Long Island Sound [*Valle-Levinson and Wilson*, 1994]. Starting from a two-layer flow, *Geyer and Farmer* [1989] suggest that vertical mixing at the salt/fresh interface creates a layer of intermediate density, which slides relative to the surface and bottom layers. Our three-layer model follows this reasoning; the middle layer represents the pycnocline and grows by parameterized entrainment from the other two layers. Parameterized bottom friction retards the lower layer, and the flood veloctity maximum is seen in the middle layer.

Circulation features like those described above may also be simulated using two- and three-dimensional numerical circulation models with turbulence closure submodels. *Valle-Levinson and Wilson* [1994] modeled tidally driven internal circulation over a sill using the Munk-Anderson scheme to model eddy viscosities and diffusivities. In the absence of vertical mixing, flood currents are strongest at the bottom. In the presence of vertical mixing a middepth maximum appears when barotropic currents are about half the internal wave speed. This occurs near the end of flood when the model is driven with moderate barotropic tidal currents and on early flood with stronger tidal currents. In the strongly forced case, peak flood currents increase monotonically toward the surface. These results are consistent with observations in the Columbia River entrance channel, which is subject to very strong barotropic currents.

Another prior study with results similar to ours is the model of *Winters and Seim* [2000]. Their three-dimensional model uses the Mellor-Yamada turbulent

Paper number 2000JC900151.
0148-0227/01/2000JC900151$09.00

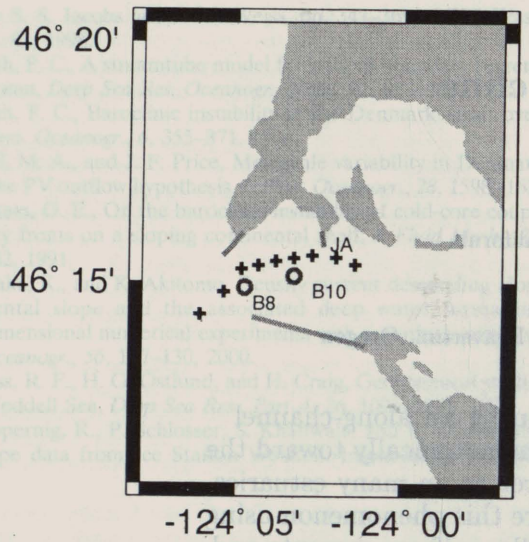

Figure 1. Map of Columbia River entrance area. The Pacific Ocean is to the left, and the estuary is to the right. Buoy 8 (B8) marks the entrance, there are wide shoals south of buoy 10 (B10), and the channel is narrowest near jetty A (JA). Time series measurements were made near buoy 10 in May 1992. Crosses mark the along-channel transect used in September and October 1995.

closure scheme to model the effects of vertical mixing in a lock exchange between salt and fresh water. An interfacial layer of intermediate density is formed by vertical entrainment and carries water away from the constriction in both directions. The shape of this interfacial layer is essentially identical to the layer developed in our simpler three-layer model. The symmetry of this three-layered circulation is broken down by bottom friction, as we also find below. The three-dimensional model validates the layer model, which may then be run quickly for a wide variety of situations.

Yet another possible approach to modeling the vertical distribution of currents is a harmonic profile model [*Ianniello*, 1977], possibly with the addition of baroclinic forcing [*Jay and Smith*, 1990a]. This method is ill suited to the Columbia River entrance channel because the flow is often supercritical with respect to the internal Froude number, violating the assumptions of the model. A fully nonlinear approach to the along-channel momentum equations is needed.

Prior studies involving three-layer models have focused more on internal hydraulics than on vertical mixing. The models of *Hogg* [1985] and *Stacey and Zedel* [1986] reveal control points, hydraulic jumps, and locations of flow blocking and separation near sills. However, neither model allows for vertical mixing between the layers, which is a fundamental part of the circulation of shallow straits and estuaries.

The present study combines the computational simplicity of a three-layer model with parameterizations for vertical mixing and bottom friction. The models of *Winters and Seim* [2000] and *Valle-Levinson and Wilson* [1994] produce results similar to ours and many other insights. By contrast, we wish to test the simplest possible explanation for the observed middepth maximum in the flood current, invoking only three forces (barotropic and baroclinic pressure gradients and bottom friction) and minimal geometry (three layers in a one-dimensional channel). The resulting model runs quickly on any platform, allowing exploration of parameter space as described by *Cudaback and Jay* [2000].

2. Observed Three-Layer Circulation

The Columbia River entrance channel, "the graveyard of the Pacific," is shown in Figure 1. This narrow

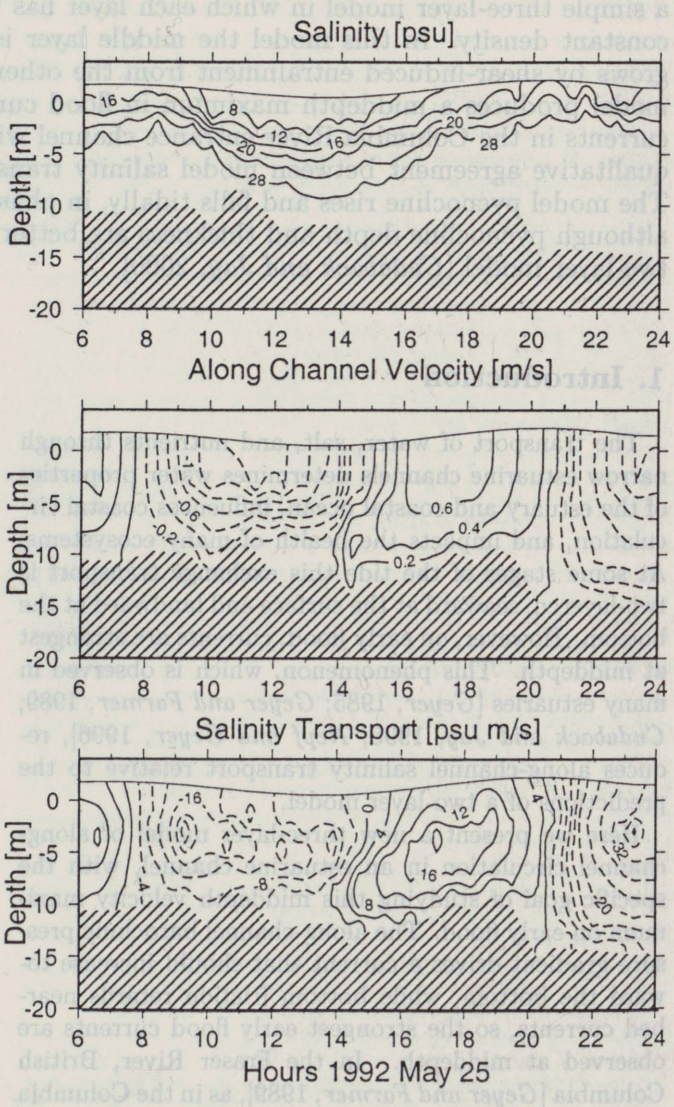

Figure 2. Time series of observed (top) salinity, (middle) currents, and (bottom) salinity transport. Axes are dimensional times and depth. The pycnocline drops and thickens on ebb, then rises and thins again on flood. Peak flood and ebb currents are strongest near the surface, but early flood currents are strongest near the bottom. Transport is thus strongest at middepth on peak flood and peak ebb.

channel on the Oregon/Washington border controls all exchange of salt and fresh water between the Columbia River and the Pacific Ocean. The simplest models of this transport are baroclinic estuarine circulation and barotropic tidal transport. Observed circulation is a combination of the two processes, with additional complications due to bottom friction and interfacial mixing.

We will consider two data sets in this paper. First, a time series of velocity and density data was collected during an 18 hour occupation of a channel cross section near buoy 10 on May 25, 1992. This location is just seaward of a lateral constriction at jetty A. Second, several along-channel sections crossing the bar were measured in September and October of 1993. Stations in these sections are marked as crosses in Figure 1. Both data sets represent periods of neap tides and relatively low river runoff [*Cudaback and Jay*, 1996]. The first data set reveals the time-varying thickness of the pycnocline; both data sets reveal currents in the pycnoncline that vary in both time and distance along the channel.

The time series of salinity in Figure 2 shows the tidal variation in pycnocline depth and thickness, as is also discussed by *Cudaback and Jay* [2000]. Time series of velocity and transport in Figure 2 reveal the tidal asymmetry of internal circulation. A two-layer frictionless model predicts that flood currents should be strongest near the bottom, and ebb currents should be strongest near the surface. Observed ebb currents are always strongest at the surface, while maximum flood currents start near the bed and move upward through the water column. There is a brief period (1400-1600 hours) during which flood currents show a middepth maximum. This vertical progression is due to a combination of steady and time-varying barotropic forces, baroclinic forces (increasing toward the bottom), and bottom friction (which retards the lowest layer). As salinity increases toward the bottom and peak along-channel currents increase toward the surface, their product, salinity transport, is strongest at middepth.

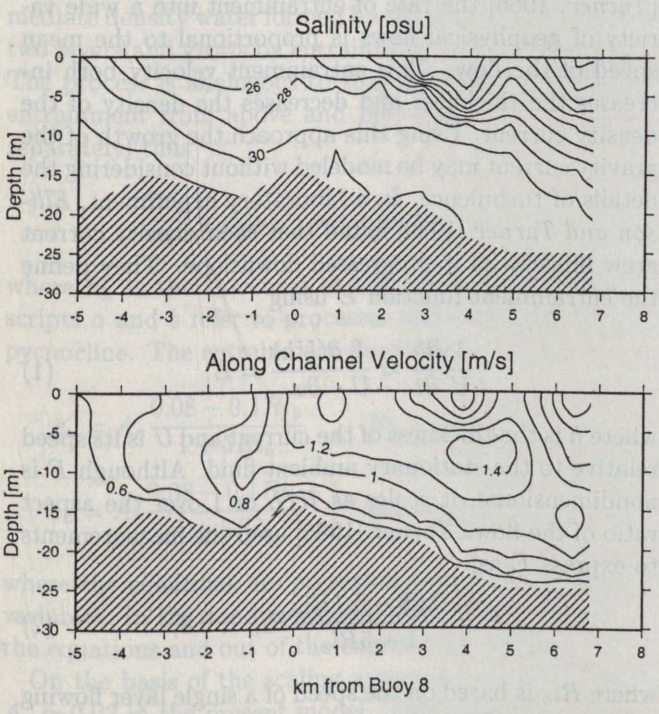

Figure 3. Along-channel section on early flood. Although the salinities (top) are roughly two-layered, the currents (bottom) show a middepth jet.

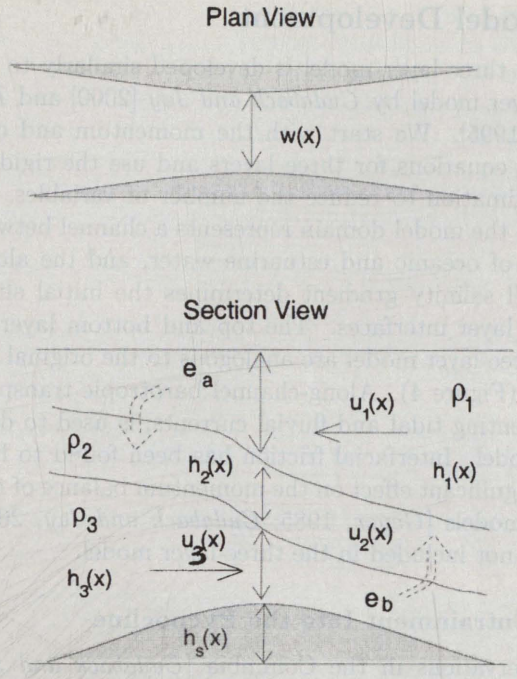

Figure 4. Definition sketch for three-layer model: (top) plan view and (bottom) section view. Layers are counted top to bottom. Layer velocities u_i and thicknesses h_i vary along-channel and with time; densities ρ_i are constant. Entrainment from the upper and lower layers into the middle layer is represented by curved arrows.

The along-channel section in Figure 3 was observed early on flood. This is the safest stage of the tidal cycle for conducting small-vessel operations, so a similar three-layer pattern of circulation and salinity is often observed. Early on flood, when an inviscid model would predict that currents should be strongest at the bottom, the strongest currents are observed in or just below the pycnocline. This middepth jet accelerates rapidly as it passes jetty A and decelerates again as the channel opens out. Although the transect pictured here lasted two hours, and is therefore not exactly synoptic, the existence and location of the middepth jet does not change over the period of the transect. Rough sea conditions precluded collection of an analogous section on ebb.

Note that the strongest middepth circulation is observed near kilometer 4, whereas the time series in Figure 2 was observed near kilometer 2, and shows a less well-developed circulation. A desire to understand this middepth jet inspired the present model study.

3. Model Development

This three-layer model is developed similarly to the two-layer model by *Cudaback and Jay* [2000] and *Helfrich* [1995]. We start with the momentum and continuity equations for three layers and use the rigid lid approximation to reduce the number of variables. As before, the model domain represents a channel between basins of oceanic and estuarine water, and the along-channel salinity gradient determines the initial shape of the layer interfaces. The top and bottom layers of the three-layer model are analogous to the original two layers (Figure 4). Along-channel barotropic transport, representing tidal and fluvial currents, is used to drive the model. Interfacial friction has been found to have an insignificant effect on the momentum balance of two-layer models [*Geyer*, 1985; *Cudaback and Jay*, 2000], and is not included in the three-layer model.

3.1. Entrainment Into the Pycnocline

Observations in the Columbia [*Cudaback and Jay*, 1996, 2000] and Fraser Rivers [*Geyer and Farmer*, 1989] show that Kelvin-Helmholtz billows on the salt/fresh interface entrain water into the pycnocline from above and below. In this model we represent the pycnocline as a layer of intermediate density created by mixing between the surface fresh layer and denser bottom layer. This middle layer grows by mass entrainment from the other two layers, but it may also shrink because of divergent along-channel advection. The layer interfaces represent isopycnals, so there is no density entrainment into the middle layer. The middle layer moves independently of the other two layers, so the model can replicate the observed middepth jet.

The symmetric entrainment into this middle layer from above and below is consistent with the approach used by *Cudaback and Jay* [2000], who found that a simple bulk Richardson number relationship could simulate the time-dependent thickness of the pycnocline. A pycnocline centered on the two-layer interface closely replicated the behavior of the observed pycnocline in the Columbia River. This result indicates that the pycnocline may grow by entrainment from the upper and lower layers equally. There are a few significant differences between the two and three-layer models. First, the pycnocline in the three-layer model has a constant density, while the pycnocline in the two-layer model has constant vertical gradients in density and velocity. Second, the pycnocline thickness in the two-layer model is estimated post facto, while the pycnocline in the three-layer model grows by entrainment at each time step.

Our situation is different from the better known case of an active layer intruding into still ambient water as a surface buoyancy current or a bottom density current. In that case, water entrains from the ambient water into the active layer, especially near the head of the active layer. The entrained water increases or reduces the density of, and continues to move with, the active layer. In the Columbia River entrance channel the conditions on early flood briefly resemble a bottom density current, and the conditions on early ebb somewhat resemble a surface buoyancy current. However, the ambient water may be considered stationary for only very brief intervals, as the tides are quite strong. Therefore we must move beyond the models with a single active layer and consider both the upper and lower layers to be active.

3.2. Continuity Equations

Pycnocline growth is modeled as entrainment from the top and bottom layers. The rate of entrainment is determined using a Richardson number dependent relationship found in the laboratory by *Ellison and Turner* [1959]. The Richardson number has stratification in the numerator representing the potential energy needed to raise a parcel of water by a certain distance. The square of the shear, in the denominator, represents the kinetic energy available to raise that parcel. Thus a large Richardson number indicates a stable water column in which the vertical exchange of momentum and mass is inhibited. If density and velocity gradients are assumed to be constant over a certain depth range, a bulk Richardson number may be used. In this paper we will use different forms of bulk Richardson number for model development and diagnostic purposes.

A bulk Richardson number, Ri_o was used by *Ellison and Turner* [1959] to develop a parameterization for entrainment into a turbulent gravity current. This current consisted of water significantly denser than ambient running down a sloped floor under the influence of gravity. According to the "entrainment hypothesis" [*Turner*, 1986] the rate of entrainment into a wide variety of geophysical flows is proportional to the mean speed of the flow. This entrainment velocity both increases the thickness and decreases the density of the density current. Using this approach the growth of the gravity current may be modeled without considering the details of turbulence. In a laboratory experiment, *Ellison and Turner* [1959] found that their density current grew linearly as it progressed downslope. They define the entrainment function E using

$$\frac{1}{U}\frac{\partial h}{\partial t} \approx \frac{1}{U}\frac{\partial (Uh)}{\partial x} = E, \tag{1}$$

where h is the thickness of the current and U is its speed relative to the stationary ambient fluid. Although E is nondimensional, it scales as H/L or 1 over the aspect ratio of the flow. *Turner* [1986] used the measurements to express E as

$$E = \frac{0.08 - 0.1Ri_o}{1 + 5Ri_o} \quad Ri_o < 0.8, \tag{2}$$

where Ri_o is based on the speed of a single layer flowing under stationary ambient fluid.

$$Ri_o = \frac{g' h \cos\theta}{U^2}, \tag{3}$$

where θ is the slope of the bottom, which is zero in an estuarine exchange flow. In this experiment, vertical entrainment stops at a critical Richardson number of 0.8. E varies between 0 and 0.08, indicating gradual growth of the density current.

The entrainment function E depends upon the aspect ratio of the flow, which must be considered in any model using this function. *Ellison and Turner* [1959] did not state the aspect ratio of their laboratory flows, but from their figures and tank dimensions it appears that $(L/H)_{ET} \approx 20 - 60$, where the subscript ET indicates their work. *Price and Baringer* [1994] successfully used (2) to model entrainment into dense outflows from marginal seas. Their model results correlated well with observations, implying that this formulation is consistent with geophysical flows. However, the aspect ratio in Price and Baringer's model is coincidentally quite similar to the aspect ratio in Ellison and Turner's experiment. By contrast, the aspect ratio of the Columbia River entrance channel is much greater, $(L/H)_{CR} \approx 500 - 1000$. The entrainment function used in the present model of the Columbia River is therefore rescaled by A_r, the ratio of $(L/H)_{ET}$ to $(L/H)_{CR}$.

$$E_{CR} \approx \frac{(L/H)_{ET}}{(L/H)_{CR}} E_{ET} = A_r E_{ET}, \tag{4}$$

where $A_r \approx 0.02 - 0.1$.

The above arguments apply to the growth of a single layer flowing by gravity under a stationary ambient layer. We use a related approach to parameterize the growth of the middle layer in the present three-layer model. The middle layer is assumed to consist of intermediate density water formed by the mixing of the other two layers and grows by entrainment from those layers. The process is analogous to that described above, but entrainment from above and below must be modeled separately; thus

$$\frac{\partial h_2}{\partial t} = e_a|u_2 - u_1| + e_b|u_3 - u_2|, \tag{5}$$

where h_2 is the thickness of the pycnocline and subscripts a and b refer to processes above and below the pycnocline. The entrainment functions are defined as

$$e_a = A_r \frac{0.08 - 0.1Ri_a}{1 + 5Ri_a}, \quad Ri_a = \frac{g' h_2}{2(u_2 - u_1)^2}, \tag{6}$$

$$e_b = A_r \frac{0.08 - 0.1Ri_b}{1 + 5Ri_b}, \quad Ri_b = \frac{g' h_2}{2(u_3 - u_2)^2}, \tag{7}$$

where the equations are presented here in dimensional variables. In the nondimensional model g' drops out of the equations and out of the expressions for Ri.

On the basis of the scaling argument above we used $A_r \approx 0.02$ in the present model. This scaling is consistent observations in the Columbia River entrance channel. The observed pycnocline grows by $\approx 10^{-4}$ m s^{-1}on ebb, whereas the maximum growth rate obtained by using Price and Baringer's value for E is $\approx 10^{-2}$ m s^{-1}. Again, the entrainment rate must be reduced by $O(10^2)$.

Note that the speed of a single layer in (2) is now replaced by the shear between adjacent layers and that the vertical scale is only half the pycnocline thickness. It should also be remembered that estuarine exchange flows are driven by along-channel barotropic and baroclinic forcing, while the density currents studied by *Ellison and Turner* [1959] are driven by gravity down a sloping bottom. The different dynamics may cause subtle differences in the turbulent entrainment between layers. Our model study tests the breadth of applicability of this entrainment function.

The above entrainment function fits into the continuity equations as follows. For the three-layer model, imagine two layers separated by a very thin interface. Vertical shear between the layers drives turbulent overturns and creates water of intermediate density. The creation of this water is represented as entrainment from the top and bottom layers into the middle layer. Mixing is irreversible; intermediate density water cannot turn back into fresh or salt water, so the vertical entrainment is one way. However, along-channel currents diverge in the middle layer [*Winters and Seim*, 2000], so the layer does not grow indefinitely. The dimensional continuity equations are

$$\frac{\partial h_1}{\partial t} = -\frac{1}{w}\frac{\partial}{\partial x}(wh_1u_1) - e_a|u_{21}|, \tag{8}$$

$$\frac{\partial h_2}{\partial t} = -\frac{1}{w}\frac{\partial}{\partial x}(wh_2u_2) + (e_a|u_{21}| + e_b|u_{32}|), \tag{9}$$

$$\frac{\partial h_3}{\partial t} = -\frac{1}{w}\frac{\partial}{\partial x}(wh_3u_3) - e_b|u_{32}|, \tag{10}$$

where layer 1 is at the surface and layer 3 is at the bottom. Vertical shears are defined as $u_{21} = u_2 - u_1$ and $u_{32} = u_3 - u_2$, where u_i is the speed of a given layer. Channel width w, layer thickness h_i, and speed u_i all vary with distance x along the channel. Entrainment functions e_a and e_b are defined above in equations 6 and 7 [*Turner*, 1986].

As total transport is conserved in the along-channel direction, we need only two continuity equations, and the choice of which to eliminate appears to be arbitrary. Numerically, however, large instabilities may develop where a given layer gets very thin ($h_i < 0.05H$). This occurs at the seaward end of the top layer and the landward end of the bottom layer; stability is preserved by solving the continuity equations for these layers. Entrainment preserves the finite thickess of the middle layer, and the total water depth is conserved.

3.3. Momentum Equations

The three-layer model requires conservation of momentum and mass in each layer, a total of six equations. By analogy with the two-layer model development [*Helfrich*, 1995; *Cudaback and Jay*, 2000], a rigid lid approximation is then used to reduce the number and complexity of the equations. To this end we ex-

press the layer speeds in terms of vertical shears u_{21} and u_{32}:

$$u_1 = u_b - (a_2 u_{21} - a_3(u_{32} + u_{21}))/A, \quad (11)$$

$$u_2 = u_b + (a_1 u_{21} - a_3 u_{32})/A, \quad (12)$$

$$u_3 = u_b + (a_1(u_{21} + u_{32}) + a_2 u_{32})/A, \quad (13)$$

where a_i are the cross sections of the individual layers and $A = a_1 + a_2 + a_3$ is the total cross section of the channel.

The dimensional equations for vertical shear in a three-layer model are

$$\frac{\partial}{\partial t}u_{21} = -\frac{\partial}{\partial x}\left(\frac{u_2^2}{2} - \frac{u_1^2}{2}\right) + g'\frac{\partial}{\partial x}(h_1), \quad (14)$$

$$\frac{\partial}{\partial t}u_{32} = -\frac{\partial}{\partial x}\left(\frac{u_3^2}{2} - \frac{u_2^2}{2}\right) + g'\frac{\partial}{\partial x}\left(\frac{\rho_1}{\rho_2}h_1 + h_2\right) - \frac{C_b|u_3|u_3}{h_3}, \quad (15)$$

where layer speeds u_i are now defined by (11) - (13). The baroclinic term has changed sign because the vertical shear is defined as $u_i - u_{i-1}$. The reduced gravity between layers 1 and 2 is $g(\rho_2 - \rho_1)/\rho_2$ and g' between layers 2 and 3 is $g(\rho_3 - \rho_2)/\rho_3$. As $\rho_2 - \rho_1 = \rho_3 - \rho_2$ and $\rho_3 - \rho_2 << \rho_3$, we only need one value of g' in the above equations. The layer interfaces are defined as isopycnals, so the layer densities and reduced gravity are constant with time.

The model may now be driven by specifying the barotropic current u_b at all times;

$$u_b(t) = u_t \sin(2\pi t/T) + u_m, \quad (16)$$

where u_t represents tidal currents, u_m are mean (riverine) currents, and $T = 12.42$ hours is the tidal period. When the model is run, both u_m and u_t are user-specified, so u_b may be zero, steady, or time-dependent. In this paper we used semidiurnal tides and a steady river flow based on our observations.

The final momentum conservation equations used in the model are (14) and (15), in which u_i are defined using (11) - (13) and 16). The continuity equations are (8) and (10), where entrainment is parameterized using (6) and (7). Only four of these equations are independent. For comparison, the two-layer problem requires only two equations.

3.4. Bottom Roughness Coefficient

Geyer [1985] estimated the bottom drag coefficient in the Fraser River, British Columbia, as $C_d = 3 \times 10^{-3}$. Used in a two-layer model of the Columbia River entrance channel [*Cudaback and Jay*, 2000], this value provides excellent agreement with observations. Bottom friction pushes the layer interface upward in the water column and reduces its vertical motion [*Pratt*, 1986]. However, the value of C_d depends on the reference depth z_m used to define it and must therefore be increased slightly for a three layer model. The depth dependence near the bed, where the flow may be approximated as a log layer is:

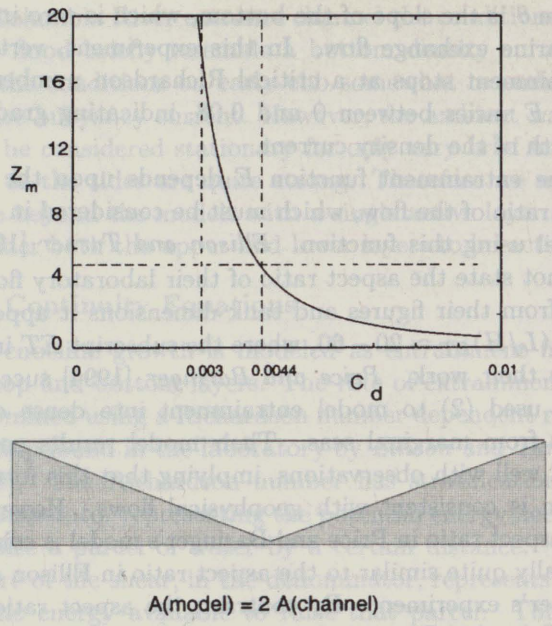

Figure 5. (top) The bottom roughness C_d decreases with distance z_m above the bottom, so $C_d(z_m = 20) = 3 \times 10^{-3}$ and $C_d(z_m = 5) = 4.4 \times 10^{-3}$. (bottom) The model channel has a rectangular cross section, with twice the area of a real triangular channel. Model currents are thus slower, and C_d must be increased to 1.2×10^{-2} for the same frictional effect.

$$C_d = \left(\frac{1}{k} ln \frac{z_m}{z_0}\right)^{-2}, \quad (17)$$

where $k = 0.41$ is von Karman's constant, $z_0 = 0.01$ m is a bottom roughness scale, and z_m is the distance above the bottom. In Figure 5 it is apparent that $C_d = 3 \times 10^{-3}$ is appropriate for a 20 m water depth. However, if the effect of bottom friction on the bottom layer alone is considered, $z_m \approx 5$m and $C_d \approx 4.4 \times 10^{-3}$. This argument is, of course, only qualitative, because of ambient stratification.

The channel cross section also affects the coefficient of bottom friction (Figure 5b). Most real estuarine channels have a trapezoidal or nearly triangular cross section, but the model channel has a rectangular cross section, making the lower layer cross section too large by roughly a factor of 2. For model transport to be equal to observed transport, model currents u_3 must therefore be half of observed currents. Bottom friction $C_d|u_3|u_3$ is quadratic in u_3, so for the same frictional effect, C_d must be multiplied by 4, giving $C_d \approx 1.2 \times 10^{-2}$. This value was used for the results that follow.

3.5. Initial Conditions

Initial conditions for the three-layer model are based on those for a two-layer model. The initial interface for the two-layer model is the steady maximal exchange so-

lution for basins of salt and fresh water at either end of the channel [*Armi and Farmer*, 1986]. In the three-layer model it is assumed that water of intermediate density is formed by mixing between the top and bottom layers. Initial model interfaces parallel the two-layer interface to represent a thin middle layer. *Helfrich* [1995] started with the surface layer moving seaward and the bottom layer moving landward. This condition is inconsistent with the strong bottom friction used in the present model, so our initial condition is still water; $u_{21} = u_{32} = 0$.

4. Model Results

Two types of preliminary model tests were made. First, the model was run to steady state in the absence of imposed barotropic currents; solutions with and without vertical entrainment are compared below. Second, the effect of time-varying barotropic (tidal) currents was studied in the absence of vertical entrainment; model results are compared with analogous two-layer model results. For all model runs a moderate channel constriction was used (Figure 6a), consistent with the Columbia River entrance channel. The channel constriction has an e-folding scale of 16 km (aspect ratio $L/H = 800$) and constricts the flow by about a factor of 3. Scale factor $\gamma = 1$ for this topography. Finally, model results are compared with observations from the Columbia River for an along-channel section on early flood and at a single location over a full tidal cycle.

4.1. Comparison With Two-Layer Model

Model results found in the absence of barotropic currents are shown in Figure 6. In the absence of vertical entrainment, the middle layer collapses, leaving a two-layer maximal exchange flow [*Armi and Farmer*, 1986]. This collapse is due to divergent along-channel advection in the middle layer and is consistent with laboratory experiments (P. MacCready, personal communication, 1998). Two-layer exchange is a natural and stable result for inviscid flow driven by a streamwise density gradient or a tilted layer interface. In the presence of vertical entrainment the model pycnocline is thin near the constriction and thick near the edges of the model domain (6c). The shape of the pycnocline is consistent with control at the constriction, while supercritical flow near the seaward end of the top layer and the landward end of the bottom layer drives rapid entrainment into the middle layer. The boundary conditions prevent hydraulic jumps. The shape of and divergent currents in the pycnocline are essentially identical to results of a three-dimensional turbulence closure model by *Winters and Seim* [2000].

Tidally forced model results without vertical entrainment are shown in Figure 7. Figures 7a – 7c show time series (four tidal cycles) of interface positions at the narrows. The strength of the forcing is different for each plot ($u_t = 0.5$, 1 and 2); all values are within the

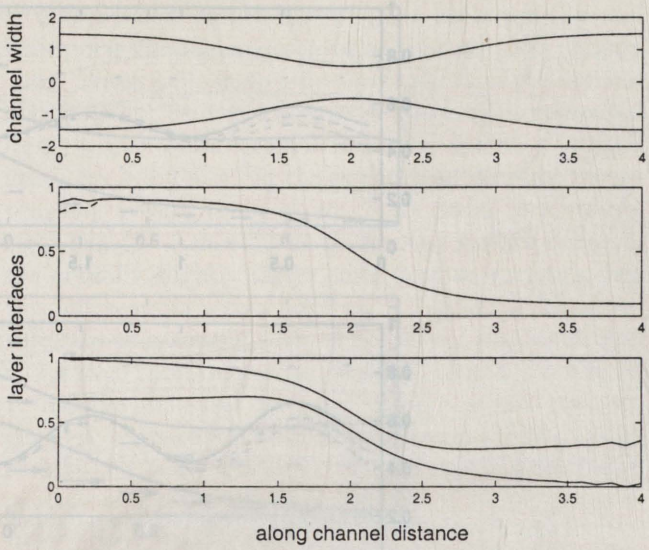

Figure 6. Three layer model results, no barotropic transport: (top) plan view of the channel and (middle and bottom) vertical sections. In the absence of vertical entrainment, the middle layer collapses, leaving a two-layer maximal exchange. Vertical entrainment is strongest near the model boundaries, and middle layer transport is divergent, so the pycnocline is thinnest at the channel constriction.

range of forcing found in the Columbia River entrance channel. For each three-layer model run the interfaces were given an initial separation of $h_2 = 0.05$, and the middle layer collapsed within one tidal cycle. After a few cycles the three-layer results (dashed lines) closely resemble two-layer results (solid lines) with similar parameters. The rapid collapse of the middle layer is due to lateral advection toward the ends of the model domain. In the two- and three-layer cases the landward and seaward migrations of the interfaces are expressed as vertical oscillation at the narrows; the oscillation increases approximately linearly with u_t. Note that even for $u_t = 2$, the interface does not reach the surface or bottom, as it would for a steady $|u_m| = 1$.

4.2. Effect of Bottom Friction

The effect of bottom friction on internal circulation was studied using the model with tidal barotropic currents and steady vertical entrainment into the pycnocline. Bottom friction breaks down the symmetry between ebb and flood circulation patterns. In the following model runs, channel topography and barotropic current strength are consistent with conditions in the Columbia River entrance channel.

Steady entrainment into the pycnocline represents the mixing between the top and bottom layers. For Figure 8 the model was run with a strong, purely tidal current ($u_t = 1.2, u_m = 0$) and no bottom friction ($C_d = 0$). For Figure 9 bottom friction was added ($C_d = 1.2 \times 10^{-2}$). In Figures 8 and 9, all subplots represent vertical sections, with the horizontal axis being

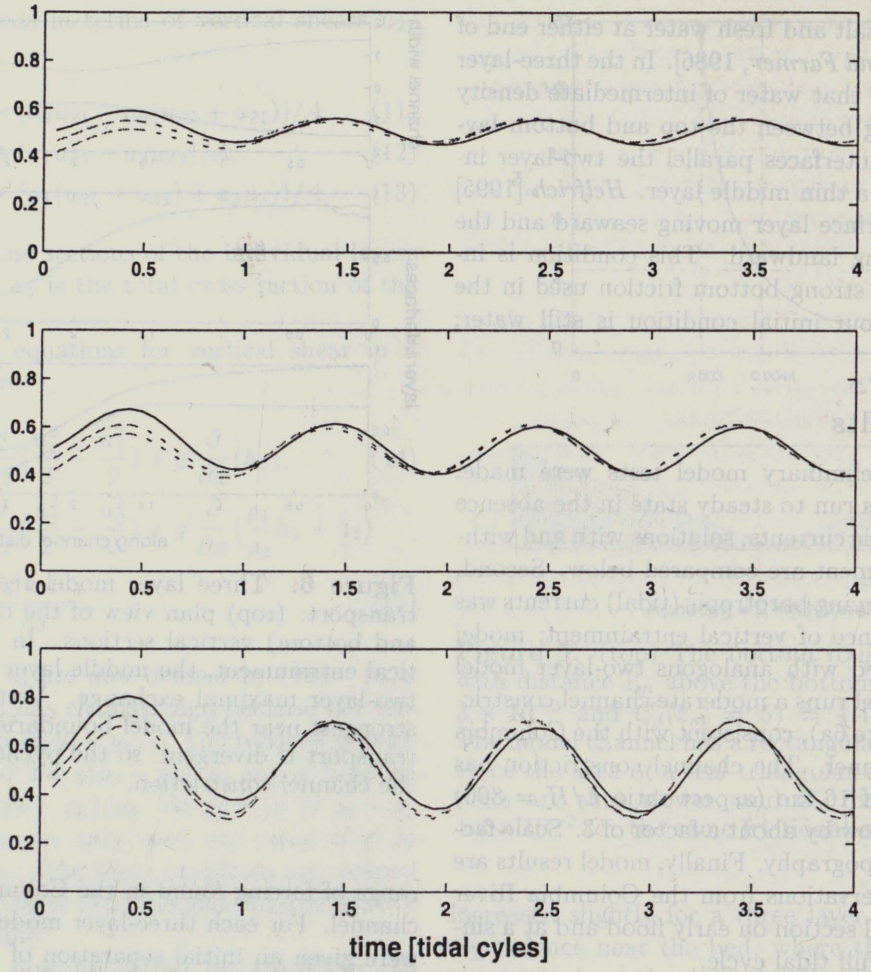

Figure 7. Three-layer model results with no entrainment into the middle layer. Dashed lines are vertical positions of layer interfaces at constriction, plotted against time. Tidal barotropic forcing u_t is 0.5, 1 and 2 in the top, middle and bottom panels, respectively. Increased forcing increases the vertical oscillation of the layer interfaces. Solid lines are the interface in an analogous two-layer model.

along-channel and fresh water to the right. The layer interfaces are overlaid with velocity vectors. Each row showa a different stage of the tidal cycle: slack water, peak flood, slack water and peak ebb, respectively.

In the absence of bottom friction (Figure 8) the overall shape of the pycnocline resembles the two-layer interface predicted by *Armi and Farmer* [1986] for a maximal exchange flow, and the whole pycnocline rises and falls slightly with the tides. The pycnocline is generally thin near the constriction and thick near the edges of the model domain, as described above [*Winters and Seim*, 2000]. The current vectors in each layer follow the tidal forcing. At both slack waters (row 1 and row 3), there is a simple two-layer exchange flow: the two circulation patterns are identical. At peak flood (row 2), currents are strongest in the bottom layer and slightly weaker in the middle layer. At peak ebb (row 4), the current profile is reversed, being strongest in the upper layer. There is clear symmetry between the flood and ebb circulation patterns.

The addition of bottom friction (Figure 9) breaks down the symmetry between flood and ebb; ebb currents are strongest at the surface, but flood currents are strongest at middepth, especially landward of the constriction. This is the middepth jet that inspired the three-layer model and cannot be replicated with a two-layer model. The whole pycnocline is also displaced upward and landward relative to the frictionless case because of reduced transport in the lower layer. This effect is also seen in the two-layer numerical model [*Cudaback and Jay*, 2000] and in the analytic model of *Pratt* [1986]. Finally, the reduced shear between layers 2 and 3 inhibits pycnocline growth, so the pycnocline is thinner near the landward end of the model domain. The tidal asymmetry shown in Figure 9 depends only on bottom friction; the addition of river flow has a relatively modest effect on internal circulation.

4.3. Tidally Averaged Transport

For comparison with observations in the Columbia River entrance channel, the model was run using a mean river flow of 0.3 m s^{-1}. Model results were calculated using the same topography and transports as above but

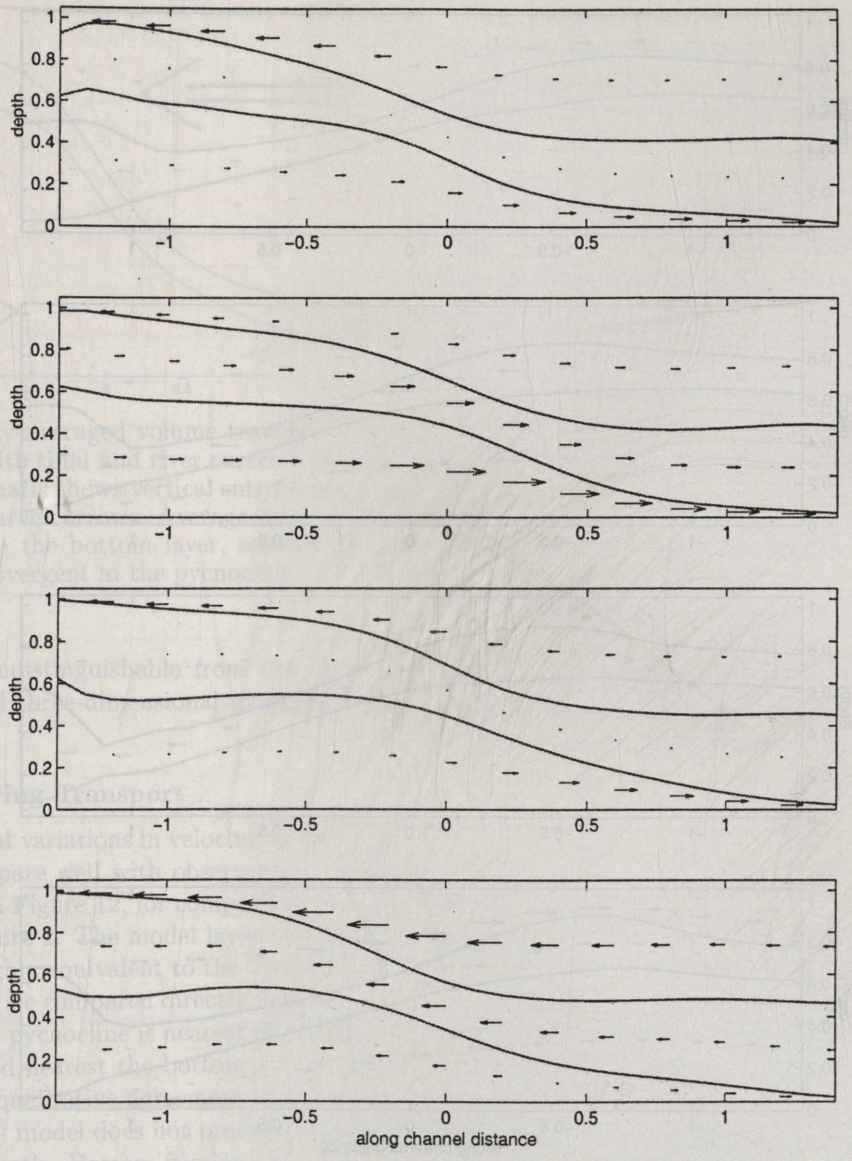

Figure 8. Three-layer model result with mass entrainment into the pycnocline, no bed friction friction ($C_d = 0$), and imposed tidal barotropic current $u_t = 1.2, u_m = 0$. Subplots are along-channel sections representing low-water slack, flood, high-water slack and ebb. Flood and ebb circulation are symmetric.

with bottom friction increased to $C_d = 1.2 \times 10^{-2}$. The internal circulation for this run is quite similar to that in Figure 9.

Tidally averaged volume transport is shown schematically in Figure 10. When tidal motions are averaged out, the pycnocline passes through the center of the model domain and is thinnest at the constriction. Transport in the middle layer is weakly divergent [*Winters and Seim*, 2000]. Average volume transport is landward in the lower layer and strongly seaward in the surface layer (straight arrows). Transport out of the estuary in the upper layer (due to river flow) is the strongest feature. Strong vertical shears drive entrainment (curved arrows) into the pycnocline from layer 1 at the seaward end of the model domain and from layer 3 at the landward end of the domain. The vertical integral of the transports in Figure 10 is total volume transport ($\sum wh_i u_i$), which varies with time but must, by the rigid lid assumption, be conserved along channel. Its tidal average is equal to the imposed mean barotropic transport $q_m = A \times u_m$. Under the rigid lid assumption, there is no Stokes drift or compensating flow.

5. Model Results Compared with Observations

5.1. Along-Channel Section on Flood

Model results with strong bottom friction and a moderate mean river flow compare well with observations. For the following discussion, $u_t = 1.2$ m s^{-1}, $u_m = -0.3$ m s^{-1}and $C_d = 1.2 \times 10^{-2}$. Along-channel sections re-

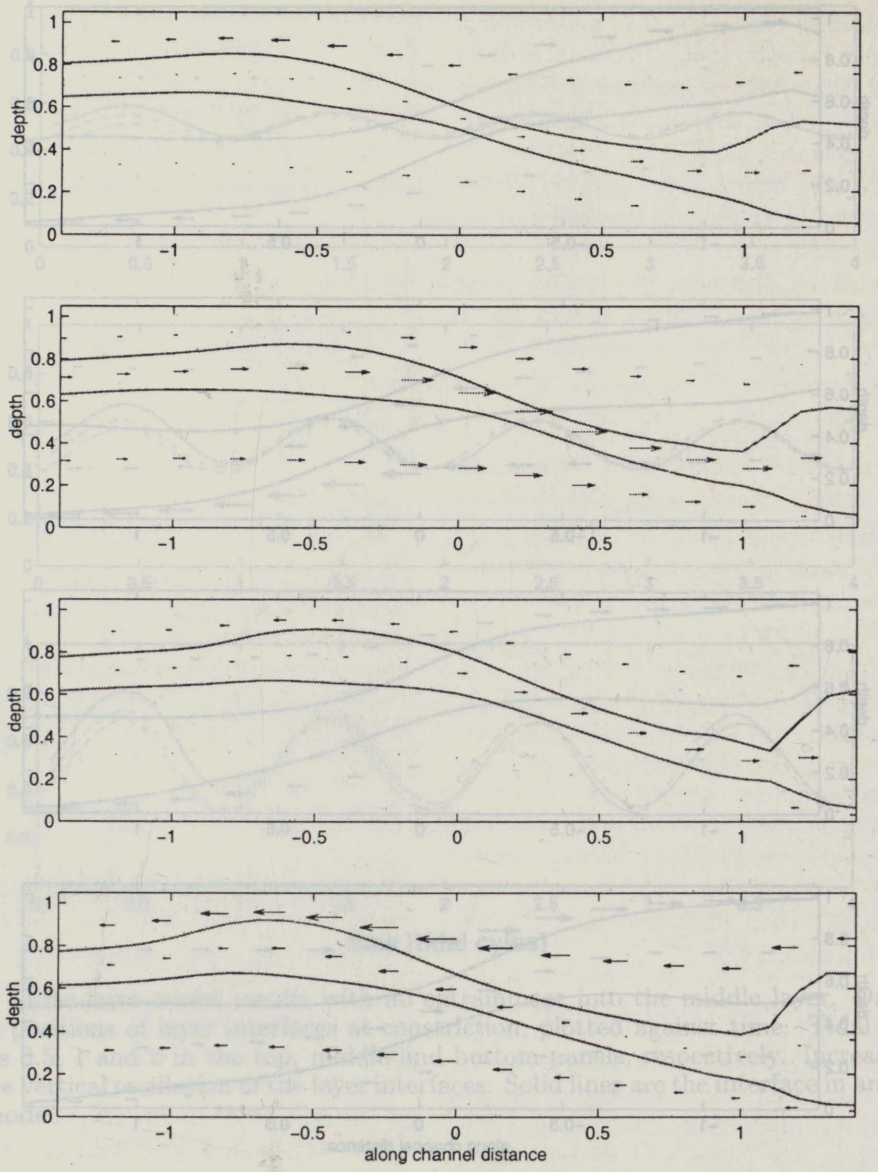

Figure 9. Three-layer model result with mass entrainment into the pycnocline, weak bottom friction $C_d = 3 \times 10^{-3}$ and imposed tidal barotropic current $u_t = 1.2, u_m = 0$. Subplots as in Figure 8. There is a middepth maximum in the flood currents, especially at the landward end of the channel. The flood/ebb symmetry has broken down.

veal a middepth maximum in early flood currents, as observed. In Figure 3a the salt wedge is advancing left to right, its top marked by the 1020 kgm^{-3} density contour. This contour is close to the surface seaward of Jetty A (2 km landward of buoy 8), and drops abruptly through the constriction, due to hydraulic control. Landward of jetty A the water remains strongly stratified, indicating the leading edge of the salt wedge. Along-channel currents (Figure 3b) are strongest at the surface just seaward of jetty A and form a plunging jet in the pycnocline landward of the constriction. The depth of maximum u is 5-10 m at jetty A and 15-20 m at km 4. Circulation landward of jetty A is essentially three-layered, with slower layers at the surface and bottom.

Model results from early flood agree qualitatively with observations (Figure 11). The pycnocline drops gently toward the landward end of the channel but is thinnest and steepest just landward of the constriction. In the absence of bottom friction the steepest drop in the pycnocline would occur at the constriction, but bottom friction pushes the whole pycnocline upward and landward [*Pratt*, 1986]. Currents are strongest at middepth and plunge landward, as observed. This simple model cannot recreate the vertical distribution of currents in detail and, specifically, cannot produce a flood jet below the pycnocline [*Valle-Levinson and Wilson*, 1994], but model results support and expand the theory of *Geyer and Farmer* [1989]. Pressure gradient forces and bottom friction are sufficient to create a middepth jet on flood. A simple three-layer model of entrainment into the pycnocline in the presence of hydraulic control results in a pycnocline shape consistent with

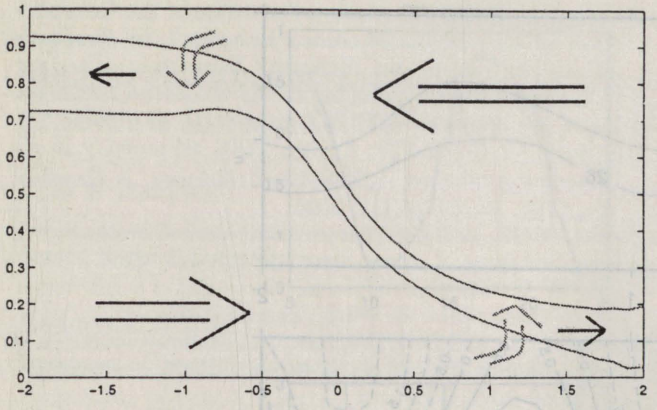

Figure 10. Tidally averaged volume transport based on model results with tidal and river currents and bottom friction. Schematic shows vertical entrainment into the pycnocline as curved arrows. Average volume transport is landward in the bottom layer, seaward in the surface layer and divergent in the pycnocline.

observations and indistinguishable from the result of a more complicated three-dimensional model [*Winters and Seim*, 2000].

5.2. Tidally Varying Transport

The modeled tidal variations in velocity, salinity, and transport also compare well with observations. Model results are shown in Figure 12, for comparison with the observations in Figure 2. The model layer interfaces in Figure 12a are roughly equivalent to the 14 and 26 psu isohalines, and may be compared directly with observations. The modeled pycnocline is nearest the surface at the end of flood and nearest the bottom at the end of ebb, in reasonable qualitative agreement with observations. However, this model does not predict the pycnocline thickness correctly. Bottom friction causes strong shear between the bottom and middle layers, especially around peak flood and peak ebb. The pycnocline grows from the bottom instead of symmetrically from top and bottom as it should [*Cudaback and Jay*, 2000]. The three-layer model is intended to replicate the middepth maximum in flood transport not the shape of the pycnocline.

The modeled time series of three-layer velocity and transports may be represented as contour plots (Figure 12b). These plots have only three points in the vertical and must not be over interpreted but may be compared directly with observations. Peak ebb currents (dashed lines) are > 1.5 m s^{-1}at the surface and decrease monotonically toward the bottom. Peak flood currents are strongest (> 1 m s^{-1}) at middepth; surface currents are actually slightly faster than bottom currents, but this difference is better resolved in Figure 13. These results are comparable with the observed maximum ebb of 1.4 m s^{-1}and maximum flood of 0.8 m s^{-1}in Figure 2. Salinity increases from the top down, and currents generally increase from the bottom up, so salinity transport ($u \times s > 24$ psu m s^{-1}) is strongest at middepth on peak ebb and peak flood, consistent with our observations and the results of *Jay and Smith* [1990b].

5.3. Bulk Richardson Number

A bulk Richardson number, calculated over the whole pycnocline thickness, is used as a model diagnostic. This form, which we will be call Ri_d, is nondimensional and may be compared directly with model results.

$$Ri_d = \frac{g'\delta z}{(\delta u)^2}, \tag{18}$$

where g' is reduced gravity, δz is the pycnocline thickness, and δu is the velocity difference across the pycnocline.

Layer velocities and bulk Richardson numbers are shown in Figure 13; observations from the Columbia are in the first column, and model results are in the second column. The 14 and 26 psu isohalines (corresponding to the model density interfaces) were used to divide the observations into three layers. When averaged over these layers, observed currents are well simulated by model results. Surface currents (solid line) range between 1 m s^{-1}landward (positive) and 2 m s^{-1}seaward (negative); seaward currents dominate in this fresh layer. Bottom currents (dashed line) are inhibited by friction and have a smaller range, about ± 0.8 m s^{-1}. Surface currents are generally more sea-

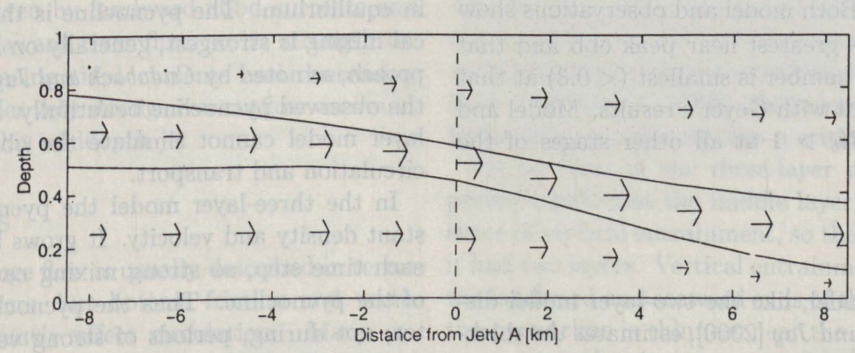

Figure 11. Model result: along-channel section on flood; fresh water is to the right. Like the observations in Figure 3, the model shows a clear middepth maximum in the currents. The pycnocline is thinnest at the constriction, and drops most steeply just landward of the constriction.

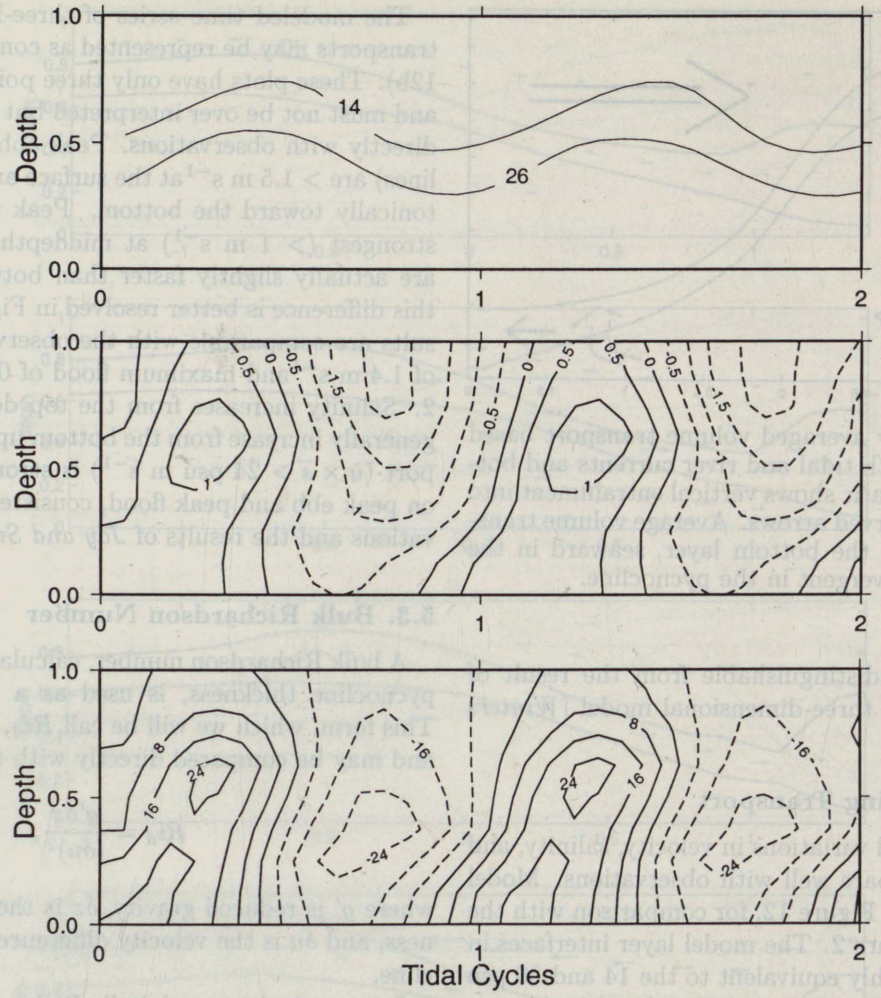

Figure 12. Time series of model results: (top) salinity, (middle) currents, and (bottom) salinity transport. The x-axes are tidal time cycles, and y-axes are non-dimensional height above the bottom. The modeled pycnocline does not replicate observations as well as the two-layer model result. Along channel currents are strongest at the surface on ebb and at middepth on peak flood. Salinity transport is strongest at middepth, as observed.

ward than bottom currents, except at peak flood, when landward surface currents are faster than bottom currents. *Geyer* [1985] measured pycnocline growth on ebb in the Fraser River; growth was inhibited at a critical value of $Ri_d \approx 0.25 - -0.33$. Similar measurements in the Columbia River indicate that Ri_d varies greatly over the tidal cycle. Both model and observations show that vertical shear is greatest near peak ebb and that the bulk Richardson number is smallest (< 0.3) at that time; this is consistent with Geyer's results. Model and observations show $Ri_b > 1$ at all other stages of the tidal cycle.

6. Discussion

The three-layer model, like the two-layer model discussed by *Cudaback and Jay* [2000], estimates the thickness of the pycnocline. However, the different approaches to the two models give significantly different results.

In the two-layer model the pycnocline is assumed to have linear vertical gradients in density and velocity. The pycnocline thickness is calculated post facto from modeled layer speeds and thicknesses. Implicit in this calculation is the assumption that the pycnocline grows quickly on a tidal time scale, so its thickness is always in equilibrium. The pycnocline is thickest when vertical mixing is strongest, generally on late ebb. This approach, as noted by *Cudaback and Jay* [2000], replicates the observed pycnocline beautifully. However, the two-layer model cannot simulate the observed three-layer circulation and transport.

In the three-layer model the pycnocline has a constant density and velocity. It grows by entrainment at each time step, so strong mixing causes rapid growth of the pycnocline. Thus the pycnocline is thickest after, not during, periods of strong vertical shear. The modeled pycnocline moves up and down in phase with the observed pycnocline but is thick when it should be thin. This difference suggests that the pycnocline thick-

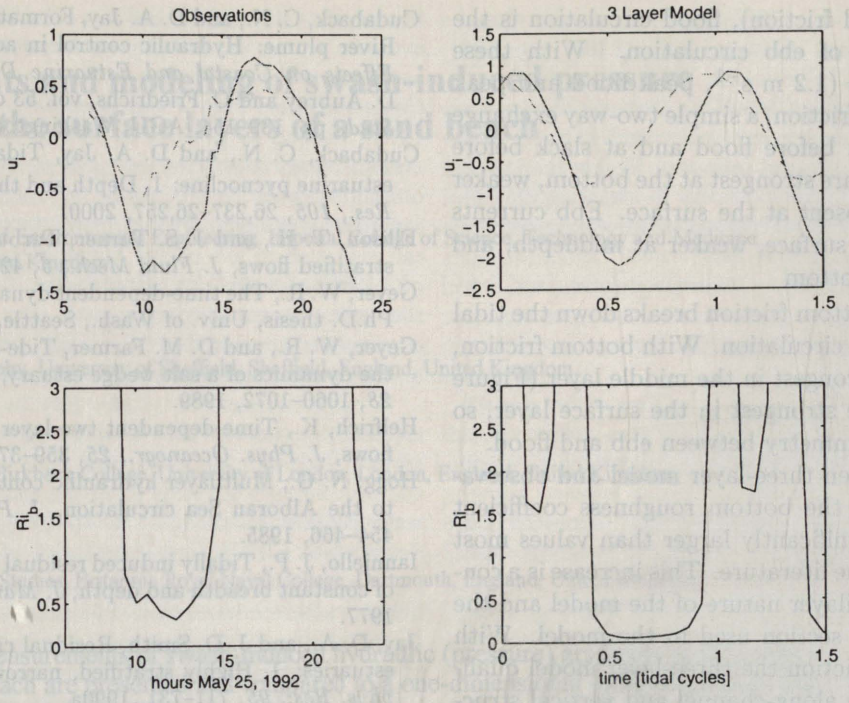

Figure 13. Time series of currents and bulk Richardson number. First column, observations; second column, three-layer model results. The modeled upper (solid line) and lower layer (dashed line) currents closely resemble observations. Ri_b is < 0.3 on ebb and > 3 on flood.

ness is best estimated by the quasi-steady methods used by *Cudaback and Jay* [2000]. However, the three-layer model still serves the very valuable purpose of explaining the observed three-layer circulation and transport.

One output of the three-layer model is tidally averaged along-channel salinity transport. Under given conditions of river outflow and tidal amplitude this average is generally nonzero. Repeated model runs show that net salinity transport is landward when river flow is weak, as was the case when our observations were collected. Later in the year, snowmelt dramatically increases the river runoff, and average salt transport is seaward. The long term salinity balance is maintained by these changing conditions.

We have also explored conditions under which a middepth jet appears on early flood. The strength of the jet $(u_2 - u_3)$ increases with increasing bottom friction. Also, the jet is driven by landward flood currents and opposed by the seaward river flux, so its strength increases with increasing tidal currents and decreasing river currents. Under very strong river outflow we would not expect to see this middepth jet.

7. Conclusions

Estuarine exchange flow is usually described in terms of two inviscid layers, but bottom friction and vertical mixing significantly affect circulation. Many estuaries have similar features [*Geyer*, 1985; *Geyer and Farmer*, 1989], but we focus on observations made in the Columbia River entrance channel. There is significant mixing between the salt and fresh layers, so the pycnocline fills 1/4 to 3/4 of the water column. It rises and falls with the tides and grows much thicker near peak flood and peak ebb. *Cudaback and Jay* [2000] found that a two-layer time-dependent model [*Helfrich*, 1995] could be modified to predict tidal variations in the position and thickness of the pycnocline.

Some aspects of observed circulation are essentially three-layered. On early flood, currents are fastest at middepth; the two-layer model cannot explain this phenomenon. In this paper we presented a new three-layer model intended to simulate these observations. The three-layer model is developed by analogy to the two-layer model, with a middle layer representing the pycnocline, which grows by shear-induced mixing. When the middle layer is very thin, strong vertical shears drive turbulent overturns and create water of intermediate density. This effect is represented by entrainment into the middle layer. The speed of entrainment is based on an empirical function of a bulk Richardson number [*Ellison and Turner*, 1959]. Entrainment stops when the Richardson number reaches a critical value of 0.8.

Initial tests of the three-layer model show the expected result that the middle layer collapses in the absence of vertical entrainment, so the model behaves as if it had two layers. Vertical entrainment is strongest near the landward and seaward ends of the model channel, so the pycnocline is thinnest near the constriction, consistent with hydraulic control at the constriction [*Winters and Seim*, 2000].

In the simplest case for the three-layer model (with-

out river flow or bed friction), flood circulation is the symmetric opposite of ebb circulation. With these purely tidal currents (1.2 m s^{-1}, peak flood and peak ebb) and no bottom friction, a simple two-way exchange flow is seen at slack before flood and at slack before ebb. Flood currents are strongest at the bottom, weaker at middepth, and absent at the surface. Ebb currents are strongest at the surface, weaker at middepth, and nonexistent at the bottom

The addition of bottom friction breaks down the tidal symmetry of internal circulation. With bottom friction, flood currents are strongest in the middle layer (Figure 9). Ebb currents are strongest in the surface layer, so there is no longer symmetry between ebb and flood.

The best fit between three-layer model and observations is found when the bottom roughness coefficient $C_d = 1.2 \times 10^{-2}$, significantly larger than values most commonly listed in the literature. This increase is a consequence of the multilayer nature of the model and the square channel cross section used in the model. With this larger bottom friction the three-layer model qualitatively recreates the along-channel and vertical structure of density and currents at most stages of the tide, including a strong middepth jet in the flood currents. These results also simulate the middepth maximum in ebb and flood salinity transport and the tidal variation in the bulk Richardson number.

Finally, we find that the salt balance in the estuary may be maintained by seasonal variations in river flow and tidal amplitude. We expect to see a significant middepth jet in any shallow estuary where tidal currents are strong relative to river flow. It will be interesting to compare these results with observations of other estuaries or of the Columbia under different conditions.

Acknowledgments. The authors are very grateful to Karl Helfrich for the use of his model code and to Parker MacCready, Arnoldo Valle-Levinson, and an anonymous reviewer for many useful suggestions. This research was supported by several grants: an Office of Naval Research graduate student fellowship, ONR grant N00014-94-1-0009 (Circulation in Stratified Tidal Channels and Straits), and National Science Foundation grants OCE-9807118 (Columbia River Land-Margin Ecosystem Research Project), and OCE-8918193 (The Columbia River Plume Project). Writing was supported by National Science Foundation grant OCE OCE96-33013. This is contribution number 27 of the Partnership for Interdisciplinary Studies of Coastal Oceans (PISCO): A Long-Term Ecological Consortium funded by the David and Lucile Packard Foundation.

References

Armi, L., and D. M. Farmer, Maximal two-layer exchange through a contraction with barotropic net flow, *J. Fluid Mech.*, *164*, 27–52, 1986.

Cudaback, C. N., and D. A. Jay, Formation of the Columbia River plume: Hydraulic control in action?, in *Buoyancy Effects on Coastal and Estuarine Dynamics*, edited by D. Aubrey and C. Friedrichs, vol. 53 of *Coastal Estuarine Stud.*, pp. 139–154, AGU, Washington, D. C., 1996.

Cudaback, C. N., and D. A. Jay, Tidal asymmetry in an estuarine pycnocline: 1, Depth and thickness, *J. Geophys. Res.*, *105*, 26,237–26,257, 2000.

Ellison, T. H., and J. S. Turner, Turbulent entrainment in stratified flows, *J. Fluid Mech.*, *6*, 423–448, 1959.

Geyer, W. R., The time-dependent dynamics of a salt wedge, Ph.D. thesis, Univ. of Wash., Seattle, 1985.

Geyer, W. R., and D. M. Farmer, Tide-induced variation of the dynamics of a salt wedge estuary, *J. Phys. Oceanogr.*, *28*, 1060–1072, 1989.

Helfrich, K., Time-dependent two-layer hydraulic exchange flows, *J. Phys. Oceanogr.*, *25*, 359–373, 1995.

Hogg, N. G., Multilayer hydraullic control with application to the Alboran Sea circulation, *J. Phys. Oceanogr.*, *15*, 454–466, 1985.

Ianniello, J. P., Tidally induced residual currents in estuaries of constant breadth and depth, *J. Mar. Res.*, *35*, 755–786, 1977.

Jay, D. A., and J. D. Smith, Residual circulation in shallow estuaries: 1, Highly stratified, narrow estuaries, *J. Geophys. Res.*, *95*, 711–731, 1990a.

Jay, D. A., and J. D. Smith, Circulation, density distribution and neap-spring transitions in the Columbia River Estuary, *Prog. in Oceanogr.*, *21*, 81–112, 1990b.

Nepf, H. M., and W. R. Geyer, Intratidal variations in stratification and mixing in the Hudson estuary, *J. Geophys. Res.*, *101*, 12,079–12,086, 1996.

Pratt, L. J., Hydraulic control of sill flow with bottom friction, *J. Phys. Oceanogr.*, *16*, 1970–1980, 1986.

Price, J. F., and M. O. Baringer, Outflows and deep water production by marginal seas, *Prog. in Oceanogr.*, *33*, 161–200, 1994.

Stacey, M. W., and L. J. Zedel, The time-dependent hydraulic flow and dissipation over the sill of observatory inlet, *J. Phys. Oceanogr.*, *16*, 1062–1076, 1986.

Turner, J. S., Turbulent entrainment: The development of the entrainment assumption, and its application to geophysical flows, *J. Fluid Mech.*, *173*, 431–171, 1986.

Valle-Levinson, A., and R. E. Wilson, Effects of sill bathymetry, oscillating barotropic forcing and vertical mixing on estuary/ocean exchange, *J. Geophys. Res.*, *99*, 5149–5169, 1994.

Winters, K. B., and H. E. Seim, The role of dissipation and mixing in an exchange flow through a contracting channel, *J. Fluid Mech.*, 2000, in press.

C. N. Cudaback, Marine Science Institute, University of California, Santa Barbara, Santa Barbara, CA, 93106. (cudaback@lifesci.ucsb.edu)

D. A. Jay, Department of Environmental Science and Engineering, Oregon Graduate Institute, 20000 NW Walker Rd, Beaverton, OR 97006-8921 USA. (djay@ese.ogi.edu)

(Received June 18, 1999; revised September 29, 2000; accepted October 12, 2000.)